Received: 3 July 2018 | Accepted: 4 January 2019

DOI: 10.1111/2041-210X.13158

RESEARCH ARTICLE

Methods in Ecology and Evolution BRITISH ECOLOGICAL SOCIETY

Population closure and the bias-precision trade-off in spatial capture–recapture

Pierre Dupont[1] | Cyril Milleret[1] | Olivier Gimenez[2] | Richard Bischof[1]

[1]Faculty of Environmental Sciences and Natural Resource Management, Norwegian University of Life Sciences, Ås, Norway

[2]CEFE, CNRS, University Montpellier, University Paul Valéry Montpellier 3, EPHE, IRD, Montpellier, France

Correspondence
Pierre Dupont
Email: pierre.dup@live.fr

Funding information
Miljødirektoratet; Naturvårdsverket

Handling Editor: Marie Auger-Méthé

Abstract

1. Spatial capture–recapture (SCR) is an increasingly popular method for estimating ecological parameters. SCR often relies on data collected over relatively long sampling periods. While longer sampling periods can yield larger sample sizes and thus increase the precision of estimates, they also increase the risk of violating the closure assumption, thereby potentially introducing bias. The sampling period characteristics are therefore likely to play an important role in this bias-precision trade-off. Yet few studies have studied this trade-off and none has done so for SCR models.
2. In this study, we explored the influence of the length and timing of the sampling period on the bias-precision trade-off of SCR population size estimators. Using a continuous time-to-event approach, we simulated populations with a wide range of life histories and sampling periods before quantifying the bias and precision of population size estimates returned by SCR models.
3. While longer sampling periods benefit the study of slow-living species (increased precision and lower bias), they lead to pronounced overestimation of population size for fast-living species. In addition, we show that both bias and uncertainty increase when the sampling period overlaps the reproductive season of the study species.
4. Based on our findings, we encourage investigators to carefully consider the life history of their study species when contemplating the length and the timing of the sampling period. We argue that both spatial and non-spatial capture–recapture studies can safely extend the sampling period to increase precision, as long as it is timed to avoid peak recruitment periods. The simulation framework we propose here can be used to guide decisions regarding the sampling period for a specific situation.

KEYWORDS
mortality, population dynamics, recruitment, spatial capture–recapture, time-to-event modelling

1 | INTRODUCTION

Spatial capture–recapture (SCR) models (Borchers & Efford, 2008; Royle & Young, 2008) are becoming increasingly popular in ecology. One of the strengths of SCR models is their ability to yield spatially explicit estimates of abundance, an important metric for conservation and management (Bischof, Brøseth, & Gimenez, 2016). At the core of SCR methods resides the concept that individual detection probability is inherently variable in space as a result of both individual space use and spatial configuration of detection devices or

monitored locations (Efford, 2014). SCR models allow estimation of the latent locations of individuals, usually defined by their home range or activity centre (Royle, Chandler, Sollmann, & Gardner, 2013), in addition to the individual latent states usually modelled in non-spatial capture–recapture (CR) models (Gimenez et al., 2007) (e.g. alive/dead for the most classic Cormack–Jolly–Seber model). This joint modelling of individual locations and states makes SCR particularly fit to analyse data collected using non-invasive monitoring methods, such as camera trapping (Royle, 2011) or non-invasive genetic sampling (NGS: Lukacs & Burnham, 2005), and explains why investigators studying wide-ranging, elusive or rare species have embraced SCR methods (Blanc, Marboutin, Gatti, & Gimenez, 2013; Sollmann et al., 2011).

Despite constant improvements in both monitoring (Harris, Thompson, Childs, & Sanderson, 2010; Lampa, Henle, Klenke, Hoehn, & Gruber, 2013; O'Connell, Nichols, & Karanth, 2010; Roon, Waits, & Kendall, 2005) and analytical methods (Muneza et al., 2017; Royle, Fuller, & Sutherland, 2017; Royle et al., 2013), studying rare and elusive species still requires considerable effort and investment by practitioners to collect sufficient data. Sparse data, that is, when the detected proportion of the population is low, lead to imprecise estimates (Otis, Burnham, White, & Anderson, 1978). This is a particularly salient issue for SCR analyses, as they require multiple detections of the same individuals at different locations in order to be able to estimate the location of latent activity centres. Lengthening the period during which data are collected (the *sampling period* hereafter) is one common way to increase the size of the dataset, thereby increasing both the proportion of individuals detected and the number of detections per individual. Occasionally in SCR studies, the sampling period can encompass a substantial part of a species' biological year (up to 39 weeks in Després-Einspenner, Howe, Drapeau, & Kühl, 2017 or even up to 376 days in Jędrzejewski et al., 2017).

On the other hand, extending the sampling period may lead to potential violations of the population closure assumption, fundamental to both spatial and non-spatial CR methods (Lebreton, Burnham, Clobert, & Anderson, 1992; Royle et al., 2013). This assumption is rarely, if ever, met in practice as some individuals may die/emigrate or new individuals are born/immigrate during the sampling period, which in turn, may change both population size and composition. Population size estimates obtained under these circumstances no longer reflect the state of the population at a given point in time, but rather a composite estimate based on the cumulative number of individuals present during the entire duration of the sampling period (Otis et al., 1978). This measure then becomes challenging to use for researchers interested in the biology of the species under study or for managers interested in population status. Most importantly, management or conservation decisions based on flawed inference may miss their goal (e.g. hunting quotas based on such "cumulative population size" might lead to overhunting).

Following this, we expect to find an optimal sampling period that balances bias and precision of estimates for a given population and monitoring setting. Previous studies that investigated this long-known limitation in the context of classical CR methods failed to detect such bias-precision trade-off and concluded instead that they were very robust to population closure violations, thus advocating for longer sampling periods to maximize the precision of estimates (Hargrove & Borland, 1994; Kendall, 1999; O'Brien, Robert, & Tiandry, 2005; Otis et al., 1978; Rota, Fletcher, Dorazio, & Betts, 2009). However, these studies only explored specific cases, such as random temporary emigration (Kendall, 1999), constant mortality rates without recruitment (O'Brien et al., 2005), or stable populations that is, when recruitment exactly counter-balances mortality (Hargrove & Borland, 1994), thus ignoring realistic scenarios where unbalanced entries and departures into/from the population might occur during sampling.

Similar to the probability to detect an individual, the probability for any given individual to leave the population (through mortality or emigration) and the probability for any new individual to enter the population (through reproduction or immigration) both increase with time. Continuous time-to-event models, which model the time until an event of interest occurs (e.g. death of a patient, failure of an engine; Klein & Moeschberger, 2005), that is the rate at which this event occurs, are well-suited to capture these processes. The rates at which individuals enter and depart from the population determine the extent to which a given dataset violates the population closure assumption and likely affect the potential trade-off between SCR estimators' bias and precision. We therefore expect the effect of sampling period duration on population size estimates returned by SCR models, as well as classical CR models, to depend on the life-history strategy of the species under study (Stearns, 1992). Finally, in many taxa, both recruitment and mortality vary throughout the year (Anderson, Rhodes, & Kator, 1983; Brockman & Schaik, 2005; Gauthier, Pradel, Menu, & Lebreton, 2001). Hence, the severity of the population closure violations is also expected to vary based on the timing of the sampling period relative to the recruitment and mortality schedules of the species considered.

The aim of this study was to quantify the consequences of violating the closure assumption for population size estimates obtained using SCR methods. Using simulations, we evaluated: (a) the consequences of extending the sampling period on population size estimates for different life histories and sampling intensities, and (b) the influence of the timing of the sampling period relative to peaks in mortality and recruitment under the same life-history scenarios. With this study, we provide practitioners with guidelines and an approach for defining an adequate sampling period for SCR studies that minimizes bias caused by the violation of the closure assumption whilst maximizing the precision of estimates.

2 | MATERIALS AND METHODS

2.1 | Time-to-event simulations

The length and timing of the sampling period are likely to determine the amount of information in the dataset as it influences the detectability of individuals in the population (e.g. Bischof et al., 2014). Both the probability for an individual to leave the population *via* death or emigration and the probability to enter the population *via*

recruitment or immigration (i.e. the biological processes) increase with time. In addition, the probability to detect an individual *given that it is alive and present in the population* (i.e. the detection process) also increases with time. In other words, the probability for an individual to be detected and enter the dataset is the result of a hierarchical time-to-event process (Klein & Moeschberger, 2005) whereby the biological processes determine the time an individual was alive and/or present in the population, which in turn conditions its detectability (Figure 1). This perspective differs from the usual way of simulating CR datasets, where the state of an individual is first modelled and then a single detection probability is applied to all individuals in a particular state (Kery & Schaub, 2011, Supporting Information 3). Using this set-up, both demographic and detection processes are instantaneous and the simulation process matches the model structure exactly. Such simulations are useful for testing a model, but their lack of realism limits our ability to draw inferences about the effect of closure violations in real-life situations (but see Bischof et al., 2014 or Ergon & Gardner, 2014 for a consideration of time-dependent detection probabilities).

In an effort to better capture the true processes in our simulations, we used three distinct functions: (a) a survival function *S(t)* describing the probability for an individual to survive/not emigrate until time *t*, (b) a reproduction function *R(t)* describing the probability for an individual to be recruited/immigrate before time *t*, and (c) a detection function *P(t)* describing the probability for an individual to be detected before time *t*. Each of these time-to-event functions *X(t)* is associated with a hazard function $h_X(t)$ describing the potential for the focal event *X* to happen *exactly* at time *t*, that is, the evolution of the intensity of the process over time (Choquet, Garnier, Awuve, & Besnard, 2017):

$$h_X(t) = -\frac{d\left(X(t)\right)/dt}{X(t)} \quad (1)$$

2.1.1 | Sampling duration

In a first analysis, we considered that all three processes—survival, reproduction and detection—occur at a constant rate throughout the year. Hence, we considered the different hazard rates h_S, h_R and h_P (survival, reproduction and detection hazard rates, respectively) to be constant over time:

$$h_S(t) = \lambda_S$$
$$h_R(t) = \lambda_R \quad (2)$$
$$h_P(t) = \lambda_P$$

The corresponding survival function is then an exponential model describing the evolution of the probability for an individual to *die after* time *t* (i.e. *survive to* time *t*):

$$S_t = e^{-\lambda_S t} \quad (3)$$

However, for the reproduction and detection processes, we are interested in the probability to reproduce or be detected *before* time *t*, not the probability to reproduce or be detected *after* time *t*. Hence, we used the complementary functions (Figure 2b):

$$\bar{R}_t = 1 - R_t = 1 - e^{-\lambda_R t} \quad (4)$$

$$\bar{P}_t = 1 - P_t = 1 - e^{-\lambda_P t} \quad (5)$$

It is worth noting that, when $\lambda_S = 0$ and $\lambda_R = 0$, all individuals survive indefinitely ($S_t = 1$) and no individual reproduces ($\bar{R}_t = 0$). This scenario corresponds to a population fulfilling the closure assumption (Figure 2a).

2.1.2 | Sampling timing

In a second analysis, we considered scenarios where both survival and recruitment hazard rates varied throughout the year following a normal distribution. This setting corresponds to the situation where most mortality and reproduction occur during a limited period of the year, as it is the case for many animal populations (Healy, 2003; Rowan, 1938):

$$h_X(t) = \frac{1}{\tau\sqrt{2\pi}} e^{-\frac{1}{2}\left(\frac{t-\mu}{\tau}\right)^2} \quad (6)$$

where μ, the mean of the normal distribution, corresponds to the mid-point of the survival or recruitment time-to-event functions,

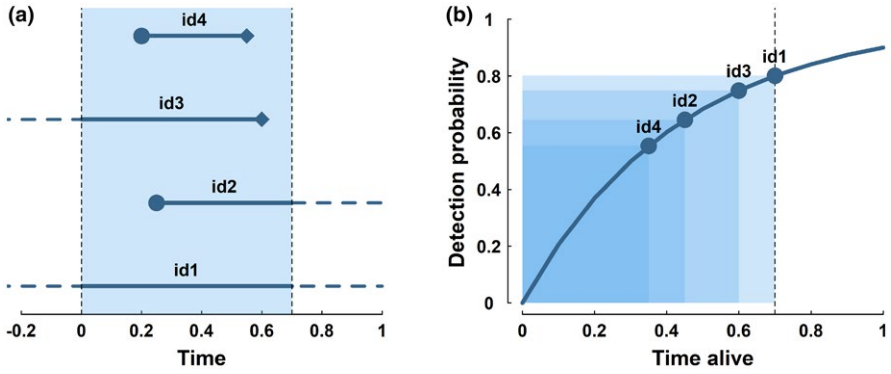

FIGURE 1 Effect of sampling duration on detection probability. (a) Biological process: four individual trajectories are shown (filled circles = birth, diamonds = death). Solid lines denote the time an individual is alive and available for detection during the sampling period (shaded area). (b) Detection process: Overall detection probability (solid line) as a function of the time alive for detection during the sampling period. The times alive and associated detection probabilities (dots) correspond to the four individuals for which availability is illustrated in panel (a)

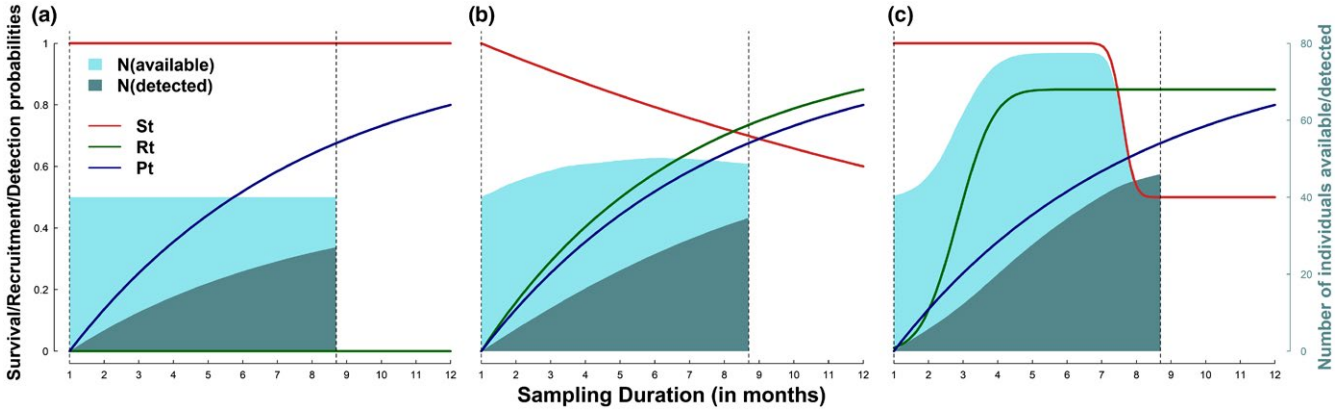

FIGURE 2 Survival S(t), recruitment R(t), and detection D(t) functions (scale on the left, solid lines); number of individuals available for detection and number of individuals detected (scale on the right, coloured polygon) for (a) a closed population, (b) a population with constant mortality and recruitment over the course of the year and (c) seasonal mortality (peak in mortality occurs during month 7) and recruitment (peak in recruitment occurs during month 3). The vertical dashed lines represent the start and end of the sampling periods

and τ, the standard deviation of the normal distribution. Under this parametrization, 95% of the mortality/reproduction occurs in the interval [μ - 1.96*τ; μ + 1.96*τ] (Figure 2c).

2.2 | SCR modelling

For the purpose of our study, we used a Bayesian approach and constructed an SCR model with data augmentation to allow for the estimation of population size (Royle & Dorazio, 2012). Our model consisted of three sub-models: (a) the spatial model, or individual point-process, which describes the distribution of individual activity centres s_i. Here, we assumed individuals to be uniformly distributed across the available habitat space H:

$$s_i \sim \text{Uniform}(H) \quad (7)$$

(b) the state model, which describes whether individual i from the augmented pool of individuals M belongs to the population of size N. This population membership is described by the state variable z_i, which takes value 1 if the individual is a member of the true population and 0 otherwise:

$$z_i \sim \text{Bernoulli}(\Psi) \quad (8)$$

where ψ is the probability for an individual from the augmented pool to belong to the population. The population size is then obtained by summing over the vector z:

$$N = \sum_{i=1}^{M} z_i \quad (9)$$

(c) the detection model, which describes the probability for an individual i to be detected at a given detector j. In this characteristic feature of SCR models, the probability to detect individual i at detector j, p_{ij} is a function of the distance d_{ij} between its activity centre s_i and the location of detector j. Here, we used the commonly used half-normal function (Borchers & Efford, 2008):

$$p_{ij} = p_0 e^{-\frac{d_{ij}^2}{2\sigma^2}} \quad (10)$$

where p_0 is the baseline detection probability and σ is the scale parameter (Royle et al., 2013).

Finally, the detection data y_{ij} is modelled as the realization of a Bernoulli process conditional on both the individual state z_i and the individual and detector-specific detection probability p_{ij} :

$$Y_{ij} \sim \text{Bernoulli}(p_{ij} z_i) \quad (11)$$

2.3 | Simulation set-up

2.3.1 | General population characteristics

We used the following settings in all simulations: (a) square habitat space of 10*10 distance units with a surrounding buffer of 2 units, (b) N = 40 individuals originally present in the population at time t_0, (c) 100 detectors regularly spaced across the habitat space (excluding the buffer area), (d) a scale parameter for the detection function σ = 1 for all individuals.

2.3.2 | Sampling duration

To account for the possible effect of the species' life history on the consequences of lengthening the sampling period, we simulated datasets following four scenarios: (a) a closed population used as reference point, (b) a long-lived species with low fecundity (e.g. African elephant *Loxodonta africana*), hereafter the slow species, (c) a species with intermediate survival and recruitment rates (e.g. red fox *Vulpes vulpes*), hereafter the intermediate species, and (d) a short-lived species with high fecundity (e.g. Montane vole *Microtus montanus*), hereafter the fast species (Table 1). For each of these four scenarios, we generated datasets for 11 different sampling period durations, t_{max}, ranging from 5% to 100% of the species annual cycle (Marra, Cohen, Loss, Rutter, & Tonra, 2015), that is, t_{max} = 0.05, 0.1, 0.2, 0.3, 0.4, 0.5, 0.6, 0.7, 0.8, 0.9 or 1 year(s). In addition, we considered different levels of sampling efficiency by testing three different detection

TABLE 1 Demographic and detection rates used in the different scenarios of the simulation study

Parameters	Closed population	Slow	Intermediate	Fast
(a) Sampling duration				
1 – Sampling period duration	$t_{max} \in [0; 1]$	$t_{max} \in [0; 1]$	$t_{max} \in [0; 1]$	$t_{max} \in [0; 1]$
2 – Survival hazard rate (λ_S)	1	0.02	0.43	1.90
3 – Reproduction hazard rate (λ_R)	0	1.90	0.51	0.1
4 – Fecundity	0	1	2	10
5 – Detection hazard rate (λ_P)	$\lambda_P \in [0.1; 0.5; 1.2]$	$\lambda_P \in [0.1; 0.5; 1.2]$	$\lambda_P \in [0.1; 0.5; 1.2]$	$\lambda_P \in [0.1; 0.5; 1.2]$
(b) Sampling timing				
1 – Sampling Period Duration	–	$t_{max} = 0.5$	$t_{max} = 0.5$	$t_{max} = 0.5$
2 – Starting Date	–	$t_{start} \in [0; 1]$	$t_{start} \in [0; 1]$	$t_{start} \in [0; 1]$
3 – Breeding season length (τ_R)	–	0.5	0.3	0.3
4 – Breeding season peak (μ_R)	–	0.4	0.3	0.4
5 – Mortality season length (τ_S)	–	2	0.2	0.3
6 – Mortality season peak (μ_S)	–	0	0	0

rates λ_P = 0.1, 0.5 and 1.2. We repeated the simulation process 100 times for each parameter configuration, leading to 13,200 simulated datasets.

2.3.3 | Sampling timing

Next, we tested the effect of the timing of the sampling period on bias and precision of SCR estimates for populations with seasonal demographic rates. Here, we only generated SCR datasets for the slow, intermediate and fast species, as the closed population has no seasonal variation in demographic rates by definition. The timing of the sampling period is therefore irrelevant in a closed population situation. Sampling duration was set to t_{max} = 0.5 year and we varied the starting date of the sampling period relative to the peaks of the reproductive and mortality periods (μ in Equation 6). This simulation study comprised 11 different starting dates (between −0.5 and +0.5 years before and after the peak in mortality) for the three life-history scenarios with 100 repetitions each, leading to 9900 simulated datasets. The different demographic rates used in the simulations are presented in Table 1.

2.3.4 | Simulation procedure

For simplicity, we refer to mortality and reproduction only in the following section, but the same procedure holds true if we were to consider emigration and immigration. The procedure for generating simulated datasets was as follows (Figure 3 and Supporting Information 1):

1. Time at death (TaD_i) for each of the N individuals present in the population at t_0 was randomly generated from the corresponding survival function S_t following Equation 3.
2. Whether and when the N original individuals reproduced (TaR_i) was determined using the corresponding reproduction function $\bar{R}_t$ (Equation 4). If $TaR_i > t_{max}$, the focal individual produced no offspring, otherwise the number of offspring (*n.off*) with time at birth equal to their parent's time at reproduction ($TaB_{n.off} = TaR_i$) was sampled from a Poisson distribution with mean fecundity F (Table 1).
3. The time at death for each offspring produced ($TaD_{n.off}$) was then sampled from the same survival function S_t as for the adults.
4. Based on the time at death, the time an individual was available for detection (T_i) was then deduced:
   - -For individuals present a t_0, T_i was set to TaD_i or to t_{max} if they survived the entire sampling period.
   - -For individuals born during the sampling period, $T_{n.off}$ corresponded to the difference between $TaD_{n.off}$ and $TaB_{n.off}$ if they died before the end of the sampling period or to the difference between t_{max} and $TaB_{n.off}$ otherwise.

   Individual baseline detection probability p_{0i} given T_i (equivalent to $\bar{P}_{it}$) was then calculated using Equation 5.
5. Individual activity centres s_i were randomly generated following Equation 7.
6. p_{ij} was then calculated using Equation 10.
7. The individual detection history y_{ij} was generated following Equation 11. Finally, we augmented the simulated dataset with all-zeros detection histories to reach a total of M = three times the number of individuals ever available for detection.

In addition to this SCR-specific simulation study, we also implemented a similar simulation approach to check for the influence of the sampling period characteristics on population size estimates returned by classical (non-spatial) CR models (Supplementary Material 3).

2.4 | Model fitting

We fit SCR models in JAGS (Plummer, 2003) through R (R Core Team, 2017) via package jagsUI (Kellner, 2015) to all simulated

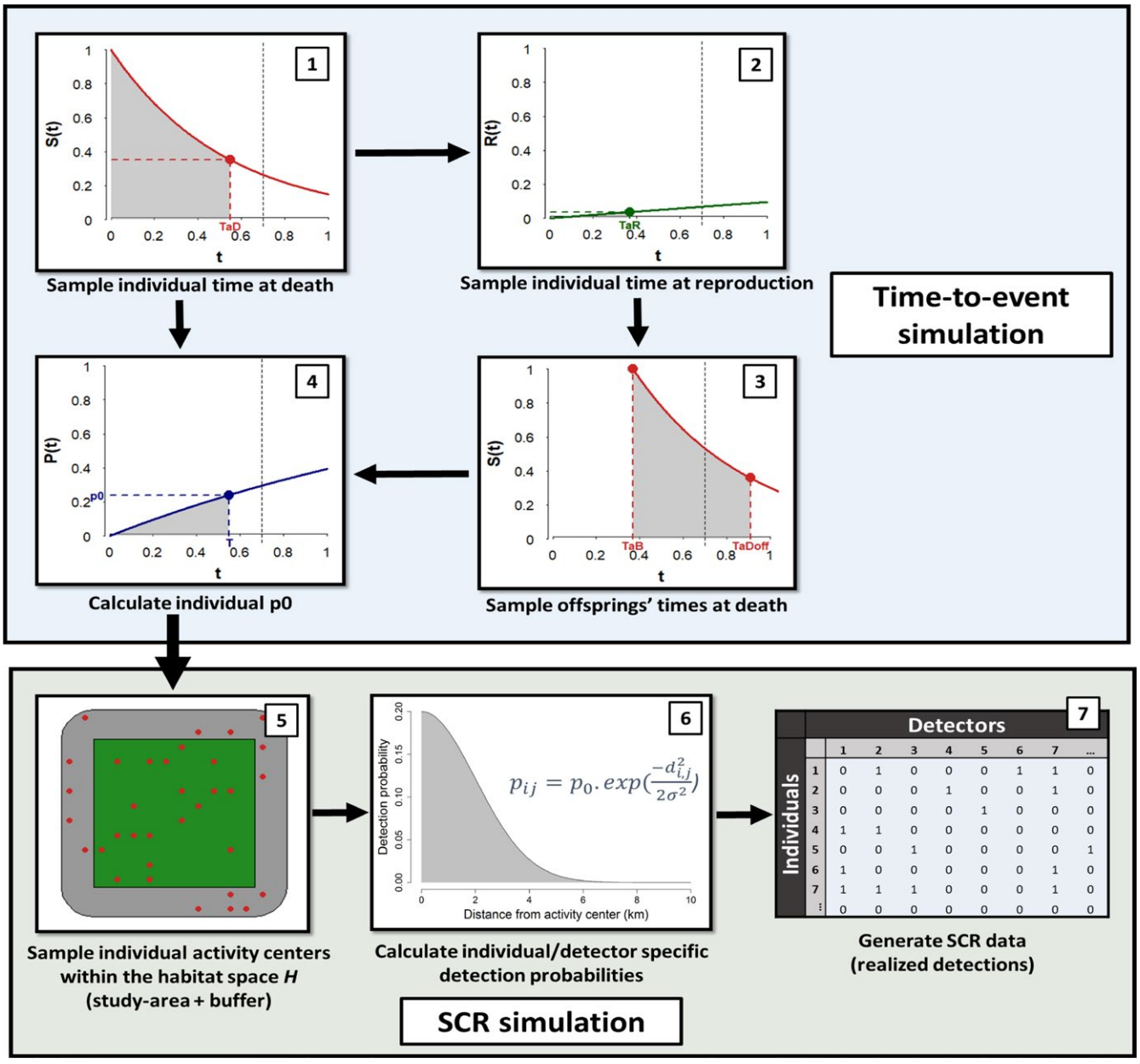

FIGURE 3 Diagram of the simulation procedure for an individual present at the beginning of the sampling period and associated offspring. The different simulation steps are described in method section 2.3.4

datasets. Three MCMC chains were run for 5000 iterations each after an adaptive phase of 1000 iterations (including burn-in). For all analyses, we considered models to have reached convergence when the potential scale reduction value Rhat < 1.1 for all parameters (Gelman & Rubin, 1992). In addition, we checked that the number of iterations was sufficient and that the different chains showed good mixing properties by visually inspecting the trace plots of the different parameters for a subset of simulations.

2.5 | Simulations evaluation

To evaluate the performance of our SCR model to recover the simulated population size under the different scenarios tested, we looked at two frequentist properties of the Bayesian estimator. As a measure of the accuracy of the SCR estimator of population size, we used the mean relative bias $\bar{B} = \sum_{j=1}^{100} \frac{\hat{N}_j - N}{100N}$, where $\hat{N}_j$ is the mode of the posterior population size distribution from the j^{th} simulated dataset and N is the true value of population size. Note that we refer to the number of individuals at the start of the sampling period in each simulation ($N = 40$) as the true population size. As a measure of precision, we used the mean over all simulations of the posterior population size standard deviation.

3 | RESULTS

All 13,200 runs for the sampling duration simulation study reached convergence. Out of the 9900 runs of the sampling timing simulation

study, only one did not reach convergence (Rhat values >1.6) and was therefore excluded from subsequent analyses.

3.1 | Closed population

When the closure assumption was met, lengthening the sampling period increased both precision and accuracy of the population size estimate returned by the SCR model (Figure 4e, i). While relative bias was around 100% for the shortest sampling periods (0.05 years), it quickly fell below 20% for sampling periods over 0.4 years when about 80% of the individuals present in the population were detected (Figure 4e). The associated standard deviation also decreased with sampling duration reaching an asymptote at approximately 3 for sampling periods over 0.4 years (Figure 4i).

3.2 | Slow life history

Similar to the results obtained for the closed population, we observed a decrease in both relative bias and standard deviation as the duration of the sampling period increased (Figure 4f,j). In addition, the timing of the sampling period did not induce noticeable additional bias or imprecision in population size estimates (Figure 5d,g). Instead, population size estimates displayed a high precision (standard deviation less than 3 for all sampling period starting dates, Figure 5g) and accuracy (relative bias below 10% for all starting dates, Figure 5d).

3.3 | Intermediate life history

Compared to the slow life history and closed population scenarios, both the number of samples and the number of individuals detected showed a more pronounced rise with increasing sampling duration for the intermediate species scenario (Figure 4c). While parameter precision increased steadily with the duration of the sampling period (Figure 4k), the relative bias first decreased before increasing again for sampling periods longer than approximately 0.4 years (Figure 4g).

In the case of seasonal peaks in mortality and recruitment, both the relative bias and standard deviation remained constant

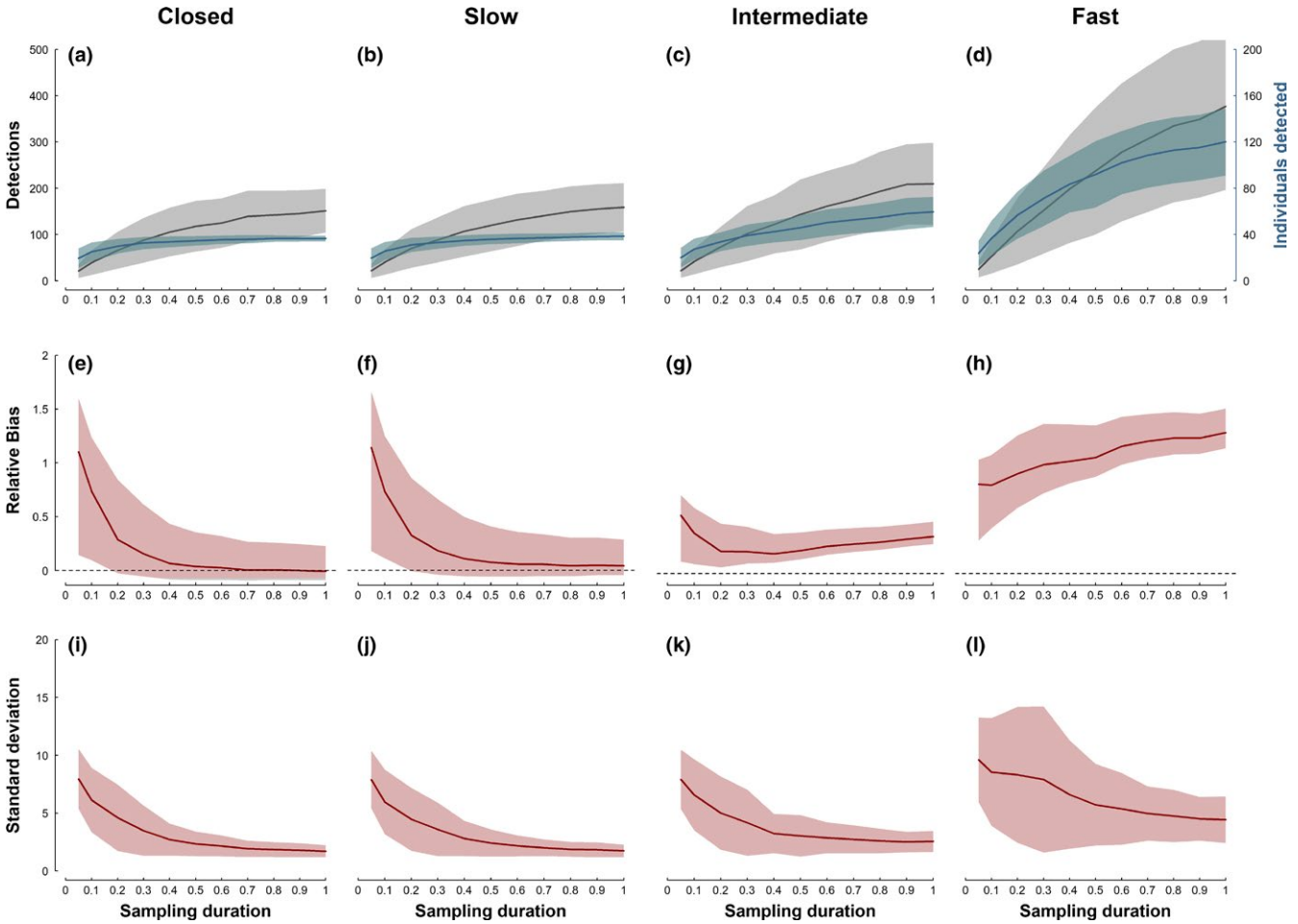

FIGURE 4 Overall number of detections (in grey, a, b, c and d), number of individuals detected (in blue, a, b, c and d), relative bias in population size estimates (in red, e, f, g and h), standard deviation of population size estimates (in red, i, j, k and l) for increasing sampling duration (*x*-axis) and different life-history strategies (left to right panel). Solid lines represent mean values over 100 repeated simulations and shaded areas represent the associated 95% confidence interval. NB: In the top row, the scales differ for the number of detections (left side) and the number of individuals detected (right side)

and relatively low as long as the sampling period did not overlap the breeding season. The relative bias then increased as the sampling period progressively overlapped the reproductive period to reach approximately 40% after the peak of the reproductive period (Figure 5e). The associated standard deviation also increased as the sampling period overlapped more and more with the reproductive period (Figure 5h).

3.4 | Fast life history

For the fast life-history strategy, the number of detected individuals was already higher than the original population size after a sampling period >0.4 years. The total number of detections also increased and was about 2.5 times higher than for the slow life-history scenario. Mean standard deviation associated with population size estimates

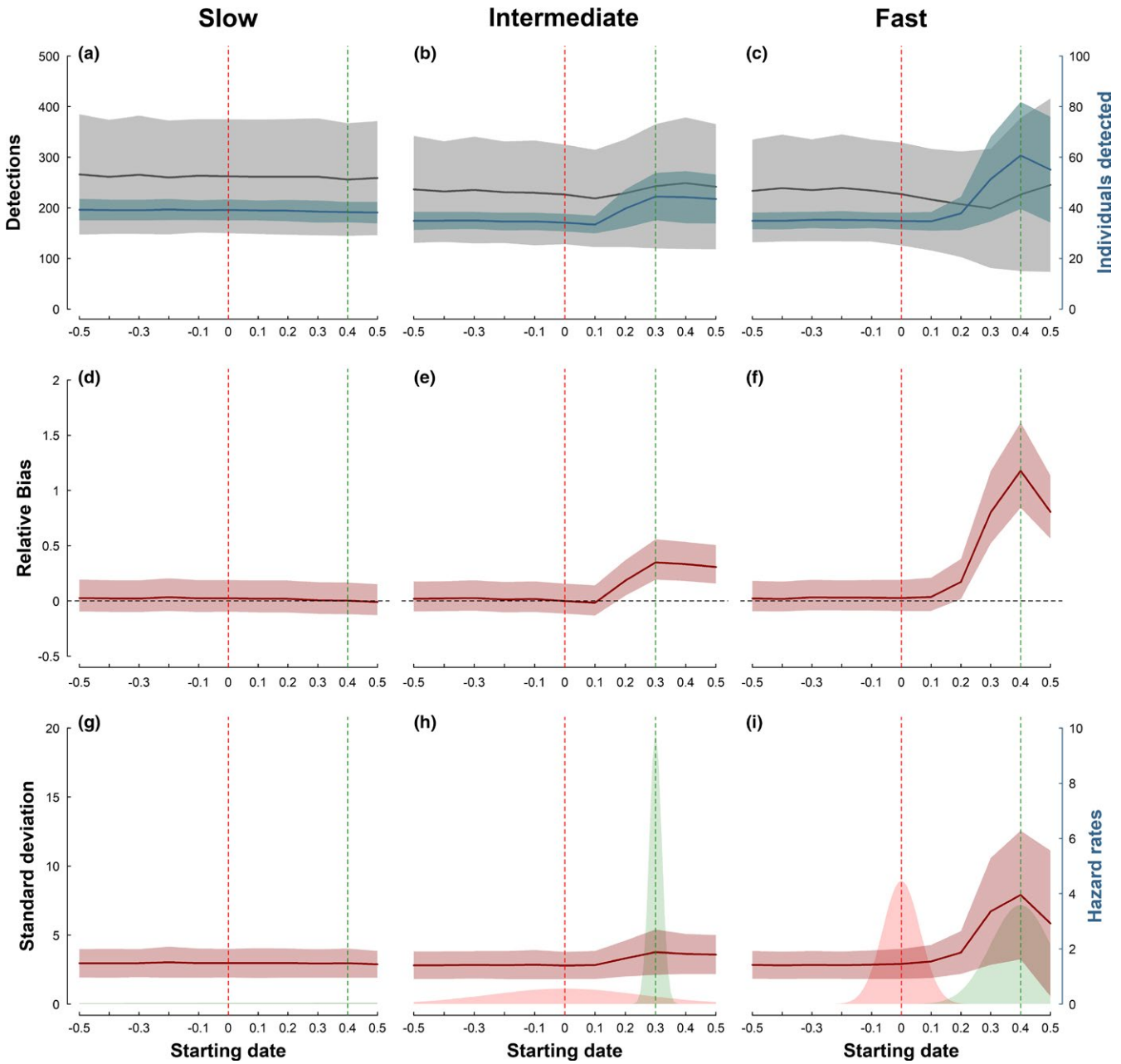

FIGURE 5 Overall number of detections (in grey, a, b and c), number of individuals detected (in blue, a, b and c), relative bias (in red, d, e and f) and standard deviation of population size estimates (in red, g, h and i) as a function of timing of the sampling period (*x*-axis) and life-history strategies (left to right panel). The timing of the sampling period is expressed relative to the peak in mortality (red vertical dashed line). The green vertical dashed line represents the peak in reproduction. Red and green Gaussian polygons represent mortality and reproduction hazard rates respectively (g, h and i). Solid lines represent mean values over 100 repeated simulations and shaded areas represent the associated 95% confidence interval. NB: In the top and bottom rows, the scales differ between the number of detections or standard deviation (left side) and the number of individuals detected or hazard rates (right side) respectively

decreased with sampling period in a fashion similar to the other simulation scenarios, albeit with greater variability as indicated by the larger standard error. Contrary to the intermediate scenario, the relative bias never decreased and instead steadily increased to reach very high levels (over 150%; Figure 4h) as soon as the sampling period exceeded 0.1 years.

Similar to the intermediate scenario, the bias in population size estimates was virtually null as long as the sampling period did not overlap the breeding season, before increasing to reach its highest level when the sampling period starting date coincided with the peak of the reproductive season (at 0.4 years; Figure 5f) before finally decreasing again. The associated standard deviation followed a similar pattern of increase and subsequent decrease (Figure 5i).

4 | DISCUSSION

We found that lengthening the sampling period during SCR studies is an effective way to increase the amount of information available for analysis, thereby boosting the precision of population size estimates. On the other hand, longer sampling periods can lead to violations of the population closure assumption and biased estimates. The shape of this bias-precision trade-off is dependent on the life-history speed and scheduling of the study species.

The gains in sample size from longer sampling periods improve the precision of abundance estimates generated by SCR models, as has also been shown for traditional CR estimators (O'Brien et al., 2005; Otis et al., 1978; Pollock, Nichols, Brownie, & Hines, 1990). Even a modest gain in terms of the number of samples collected and individuals detected can lead to a pronounced gain in the estimator's precision. We found, for example, that doubling the sampling period from 0.1 to 0.2 years brought along between 20% and 55% increase in the number of individuals detected and between 69% and 100% increase in the overall number of detections in our closed population and fast life-history scenarios respectively. The subsequent boost in the precision of the population size estimator is not trivial; it increased by 78%, 76%, 72% and 10% for the closed, slow, intermediate and fast-living scenarios respectively.

In addition to gains in precision, we also found that increased sample size can reduce bias associated with sparse SCR data. This is consistent with previous findings for classical capture–recapture methods (Chao, 1989, Supplementary Material 3). Specifically, Chao showed that the amount of bias in CR population size estimators obtained using Bayesian methods was sensitive to the choice of priors. Akin to this, the large overestimation we observed for shorter sampling periods is most likely the result of our choice of the augmented population size *M*. When data are sparse, it contains very little information and the resulting posterior distribution of the population size estimates is mostly influenced by its prior distribution (here, a flat prior between 0 and *M* = three times the total number of individuals ever available for detection). More specifically, when data are sparse, the distribution of the population size bias is skewed towards high values (Figure 4), indicating that the population size estimates returned by SCR models are constrained by the upper possible bound (i.e. the augmented population size *M*). Interestingly, this pattern seems to be even more pronounced for non-spatial capture–recapture models (Supplementary Material 3). Our findings regarding the benefits of longer study periods have important implications, especially for rare and elusive species often targeted by SCR studies (Gray & Prum, 2012), as their study tends to be hampered by data sparsity due to rarity and low detection probabilities. Furthermore, these are the species—data deficient and often threatened—where improvements in our ability to make inferences are particularly consequential, as they can inform sustainable management and conservation (Blanc et al., 2013; Gervasi, Ciucci, Boulanger, Randi, & Boitani, 2012).

The downside of longer sampling durations is the increasing risk of violating the population closure assumption. Our results suggest that studies targeting species with slow life histories (or temporarily closed populations) are largely immune to the potential biasing effect of population closure violations, whereas long sampling periods can lead to flawed inference in studies targeting species with high and intermediate life-history speeds. Our study also revealed that the positive bias induced by closure violation is primarily due to recruitment. In contrast, previous studies exploring the effect of closure violations on CR predictions focused almost exclusively on departures from the population (mortality/emigration) during sampling. This may explain the existing notion that CR methods were relatively robust to closure violations (Hargrove & Borland, 1994; Kendall, 1999; O'Brien et al., 2005; Rota et al., 2009, but see the discussion in Otis et al., 1978). In our study, where both recruitment and mortality were considered, we detected biases in population size of up to 300% when using year-long sampling periods to study species with fast-paced life histories (Figure 4h; Supporting Information 3).

In natural populations, both recruitment and mortality often peak during limited periods of the year (such as breeding and hunting seasons; Marra et al., 2015). The severity of closure violation is therefore influenced not only by the duration, but also by the timing of the sampling period relative to the focal species' annual cycle. Our simulations revealed that the timing of the sampling period relative to the mortality period had little impact on the SCR estimators' bias, probably because, for the length of sampling period and mortality rates considered here, most individuals were detected before they died (see also O'Brien et al., 2005). For the same reason, the timing of the sampling period relative to the mortality period also seems to have limited impact on the SCR estimators' precision. Conversely, sampling periods that included the peak in recruitment led to marked increases in both bias and imprecision of the population size estimator (Figure 5). The increased bias is consistent with a general loss in accuracy associated with a misrepresentation of the temporal scope of the population size estimate (e.g. a snapshot of abundance vs. the total number of individuals alive at any time during a given interval). On the other hand, the loss in precision seems at first counterintuitive: we would expect the larger sample size associated with more individuals available for detection to have the opposite effect. However, new individuals enter the dataset only for a short period of time (especially when recruitment

falls into the tail-end of the sampling period), which might increase the number of individuals detected but not the average number of detections per individual. In fact, we found that the average number of detections per individual during the sampling period decreases, as can be seen from the decrease in the total number of detections and concomitant increase in the number of individuals detected as the sampling period increasingly overlaps the recruitment season (Figure 5a, b and c; Supplementary Material 3). The minor increase in standard deviation of population size estimates observed for sampling periods overlapping the peak in mortality likely originates from the same phenomenon. As more individuals die during the sampling period, their probability of being detected multiple times declines. Hence, the average number of detections per individual decreases with an increasing overlap between the sampling period and mortality season.

In real-life situations, it may be possible to account for this type of issue even when the sampling period includes the recruitment season. Certain monitoring methods—for example camera trapping, direct observations or physical captures—allow direct identification of new recruits, such as juvenile individuals. These can then either be accounted for in the analysis, using age-specific detection functions or excluded from it. Other methods (e.g. NGS) may not allow for the identification of new juvenile recruits when they enter the population during the sampling period (but see Stenglein, Waits, Ausband, Zager, & Mack, 2011; Woodruff, Johnson, & Waits, 2016). Also, other types of new recruits (e.g. immigrating adults) may not be distinguishable from the rest of the population. Failing such distinction, investigators should strive to time the sampling period to fall outside peak seasons of recruitment (Brøseth, Flagstad, Wärdig, Johansson, & Ellegren, 2010).

Another potential limitation of our study is related to the space use of juvenile individuals. In our simulations, we did not account for the fact that juveniles often stay associated with their parents until they are weaned. This association might be negligible for short-lived species in which juveniles become independent quickly, but could be problematic for long-lived species where parents-offspring association can last longer (e.g. around 1–2 years in many large mammals; Bischof et al., 2018). This would then result in violations of the assumption of independence between individuals' activity centres. However, this particular situation is probably not problematic, as far as population size inferences are concerned, since SCR methods have been shown to be comparatively robust to the violation of independent individual placement (López-Bao et al., 2018).

The time-to-event approach we employed here enabled capturing short-term population dynamics and their repercussions for inferences drawn from realistic, non-instantaneous, sampling periods. Investigators can emulate our simulation framework in order to guide decisions regarding the length and timing of the sampling period for their specific situation. Moreover, this approach can be easily adapted to incorporate greater realism, for example by accounting for variable sampling effort over time, a common feature of many monitoring programs. This can be accomplished by allowing time varying detection hazard rates (e.g. in the same way as the survival and reproduction hazard rates, see Supporting Information 1). Similarly, the survival hazard rate function could also be modified to account for the age of the individuals at the time they enter the population. This would allow mimicking the typical situation (especially for long-lived species) where juveniles have lower survival rates than individuals old enough to breed (Promislow & Harvey, 1990). Finally, the time-to-event approach presented here proved useful to generate realistic data and test the robustness of SCR and CR methods to violations of the population closure assumption, but one could also consider continuous time capture–recapture models to study such continuous processes. Despite a great potential for application in capture–recapture studies, this framework has not been widely used so far (but see Choquet, Viallefont, Rouan, Gaanoun, & Gaillard, 2011 or more recently Ergon, Borgan, Nater, & Vindenes, 2018), and we encourage further studies to consider this analytical framework.

5 | CONCLUSION

Facing the need for large sample sizes and the desire to minimize population closure violations, how should investigators design their sampling period in SCR studies? Using a time-to-event approach, we were able to identify the bias-precision trade-off inherent in the choice of the sampling period, which was mediated by the life-history characteristics of the species under study. We therefore encourage researchers/wildlife managers to pay particular attention to the biology of their study species when designing sampling protocols. Our results show that lengthening the data collection period is an effective way to increase the number of detections, which can then lead to substantial improvements in the precision of estimates and in some cases make meaningful analyses possible in the first place. Violations of the population closure assumption arising from longer sampling durations have negligible consequences for long-lived species at the slow end of the slow-fast life-history continuum. This is an important and reassuring finding, as these are often the species with the greatest need for conservation and thus reliable information about population status. Although closure violations have more pronounced consequences for SCR inference for species with fast-paced life histories, investigators can often mitigate these by using sampling durations that balance precision and bias, and by avoiding periods of peak recruitment during sampling. Based on the patterns we observed in this study, we argue that a general rule of thumb should be to extend the sampling period as much as practically/economically feasible, while avoiding sampling during recruitment bouts.

ACKNOWLEDGEMENTS

This work was funded by the Norwegian Environment Agency (Miljødirektoratet) and the Swedish Environmental Protection Agency (Naturvårdsverket). We would also like to thank Marie Auger-Méthé, Dan Linden and an anonymous reviewer for commenting on

earlier versions of the manuscript and C. Bonenfant for his help with running the numerous simulations.

AUTHOR'S CONTRIBUTIONS

P.D., C.M., and R.B. conceived and designed the study. P.D. implemented the analysis with contributions from C.M., O.G. and R.B. All authors contributed to writing the manuscript and gave final approval for publication.

DATA ACCESSIBILITY

Data deposited in the Dryad Digital Repository http://datadryad.org/resource/doi:10.5061/dryad.t2k5143 (Dupont et al., 2019)

ORCID

Pierre Dupont https://orcid.org/0000-0002-7438-7995
Cyril Milleret https://orcid.org/0000-0002-8563-981X
Olivier Gimenez https://orcid.org/0000-0001-7001-5142
Richard Bischof https://orcid.org/0000-0002-1267-9183

REFERENCES

Anderson, I. C., Rhodes, M. W., & Kator, H. I. (1983). Seasonal variation in survival of Escherichia coli exposed in situ in membrane diffusion chambers containing filtered and nonfiltered estuarine water. *Applied and Environmental Microbiology*, *45*(6), 1877–1883.

Bischof, R., Bonenfant, C., Rivrud, I. M., Zedrosser, A., Friebe, A., Coulson, T., & Swenson, J. E. (2018). Regulated hunting re-shapes the life history of brown bears. *Nature Ecology & Evolution*, *2*(1), 116–123. https://doi.org/10.1038/s41559-017-0400-7

Bischof, R., Brøseth, H., & Gimenez, O. (2016). Wildlife in a politically divided world: insularism Inflates estimates of brown bear abundance: Transboundary wildlife populations. *Conservation Letters*, *9*(2), 122–130. https://doi.org/10.1111/conl.12183

Bischof, R., Hameed, S., Ali, H., Kabir, M., Younas, M., Shah, K. A., & Nawaz, M. A. (2014). Using time-to-event analysis to complement hierarchical methods when assessing determinants of photographic detectability during camera trapping. *Methods in Ecology and Evolution*, *5*(1), 44–53. https://doi.org/10.1111/2041-210X.12115

Blanc, L., Marboutin, E., Gatti, S., & Gimenez, O. (2013). Abundance of rare and elusive species: Empirical investigation of closed versus spatially explicit capture-recapture models with lynx as a case study. *The Journal of Wildlife Management*, *77*(2), 372–378. https://doi.org/10.1002/jwmg.453

Borchers, D. L., & Efford, M. G. (2008). Spatially explicit maximum likelihood methods for capture-recapture studies. *Biometrics*, *64*(2), 377–385. https://doi.org/10.1111/j.1541-0420.2007.00927.x

Brockman, D. K., & van Schaik, C. P.. (2005). *Seasonality in primates: Studies of living and extinct human and non-human primates*. Cambridge, UK: Cambridge University Press.

Brøseth, H., Flagstad, Ø., Wärdig, C., Johansson, M., & Ellegren, H. (2010). Large-scale noninvasive genetic monitoring of wolverines using scats reveals density dependent adult survival. *Biological Conservation*, *143*(1), 113–120. https://doi.org/10.1016/j.biocon.2009.09.012

Chao, A. (1989). Estimating population size for sparse data in capture-recapture experiments. *Biometrics*, *45*(2), 427–438. https://doi.org/10.2307/2531487

Choquet, R., Garnier, A., Awuve, E., & Besnard, A. (2017). Transient state estimation using continuous-time processes applied to opportunistic capture–recapture data. *Ecological Modelling*, *361*(Supplement C), 157–163. https://doi.org/10.1016/j.ecolmodel.2017.08.001

Choquet, R., Viallefont, A., Rouan, L., Gaanoun, K., & Gaillard, J.-M. (2011). A semi-Markov model to assess reliably survival patterns from birth to death in free-ranging populations: Survival patterns from birth to death. *Methods in Ecology and Evolution*, *2*(4), 383–389. https://doi.org/10.1111/j.2041-210X.2011.00088.x

Després-Einspenner, M.-L., Howe, E. J., Drapeau, P., & Kühl, H. S. (2017). An empirical evaluation of camera trapping and spatially explicit capture-recapture models for estimating chimpanzee density. *American Journal of Primatology*, *79*(7), e22647. https://doi.org/10.1002/ajp.22647

Dupont, P., Milleret, C., Gimenez, O., & Bischof, R. (2019). Data from: Population closure and the bias-precision trade-off in Spatial Capture-Recapture. *Dryad Digital Repository*, https://doi.org/10.5061/dryad.t2k5143

Efford, M. G. (2014). Bias from heterogeneous usage of space in spatially explicit capture–recapture analyses. *Methods in Ecology and Evolution*, *5*(7), 599–602. https://doi.org/10.1111/2041-210X.12169

Ergon, T., Borgan, Ø., Nater, C. R., & Vindenes, Y. (2018). The utility of mortality hazard rates in population analyses. *Methods in Ecology and Evolution*, *9*(10), 2046–2056. https://doi.org/10.1101/216739

Ergon, T., & Gardner, B. (2014). Separating mortality and emigration: Modelling space use, dispersal and survival with robust-design spatial capture–recapture data. *Methods in Ecology and Evolution*, *5*(12), 1327–1336. https://doi.org/10.1111/2041-210X.12133

Gauthier, G., Pradel, R., Menu, S., & Lebreton, J.-D. (2001). Seasonal survival of greater snow geese and effect of hunting under dependence in sighting probability. *Ecology*, *82*(11), 3105–3119. https://doi.org/10.1890/0012-9658(2001) 082[3105:SSOGSG]2.0.CO;2

Gelman, A., & Rubin, D. B. (1992). Inference from iterative simulation using multiple sequences. *Statistical Science*, *7*(4), 457–472. https://doi.org/10.1214/ss/1177011136

Gervasi, V., Ciucci, P., Boulanger, J., Randi, E., & Boitani, L. (2012). A multiple data source approach to improve abundance estimates of small populations: The brown bear in the Apennines, Italy. *Biological Conservation*, *152*, 10–20. https://doi.org/10.1016/j.biocon.2012.04.005

Gimenez, O., Rossi, V., Choquet, R., Dehais, C., Doris, B., Varella, H., & Pradel, R. (2007). State-space modelling of data on marked individuals. *Ecological Modelling*, *206*(3–4), 431–438. https://doi.org/10.1016/j.ecolmodel.2007.03.040

Gray, T. N. E., & Prum, S. (2012). Leopard density in post-conflict landscape, Cambodia: Evidence from spatially explicit capture-recapture. *The Journal of Wildlife Management*, *76*(1), 163–169. https://doi.org/10.1002/jwmg.230

Hargrove, J. W., & Borland, C. H. (1994). Pooled population parameter estimates from mark-recapture data. *Biometrics*, *50*(4), 1129–1141. https://doi.org/10.2307/2533449

Harris, G., Thompson, R., Childs, J. L., & Sanderson, J. G. (2010). Automatic storage and analysis of camera trap data. *The Bulletin of the Ecological Society of America*, *91*(3), 352–360. https://doi.org/10.1890/0012-9623-91.3.352

Healy, J. D. (2003). Excess winter mortality in Europe: A cross country analysis identifying key risk factors. *Journal of Epidemiology & Community Health*, *57*(10), 784–789. https://doi.org/10.1136/jech.57.10.784

Jędrzejewski, W., Puerto, M. F., Goldberg, J. F., Hebblewhite, M., Abarca, M., Gamarra, G., & Schmidt, K. (2017). Density and population structure of the jaguar (Panthera onca) in a protected area of Los Llanos, Venezuela, from 1 year of camera trap monitoring. *Mammal Research*, *62*(1), 9–19. https://doi.org/10.1007/s13364-016-0300-2

Kellner, K. (2015). jagsUI: *A Wrapper Around Rjags to Streamline JAGS Analyses*. *R Package Version*, *1*(1). Retrieved from https://CRAN.R-project.org/package=jagsUI.

Kendall, W. L. (1999). Robustness of closed capture-recapture methods to violations of the closure assumption. *Ecology*, *80*(8), 2517. https://doi.org/10.2307/177237

Kery, M., & Schaub, M. (2011). *Bayesian population analysis using WinBUGS: A hierarchical perspective*. Cambridge, UK: Academic Press.

Klein, J. P., & Moeschberger, M. L. (2005). *Survival analysis: Techniques for censored and truncated data*. New York, NY: Springer Science & Business Media.

Lampa, S., Henle, K., Klenke, R., Hoehn, M., & Gruber, B. (2013). How to overcome genotyping errors in non-invasive genetic mark-recapture population size estimation—A review of available methods illustrated by a case study. *The Journal of Wildlife Management*, *77*(8), 1490–1511. https://doi.org/10.1002/jwmg.604

Lebreton, J.-D., Burnham, K. P., Clobert, J., & Anderson, D. R. (1992). Modeling survival and testing biological hypotheses using marked animals: A unified approach with case studies. *Ecological Monographs*, *62*(1), 67–118. https://doi.org/10.2307/2937171

López-Bao, J. V., Godinho, R., Pacheco, C., Lema, F. J., García, E., Llaneza, L., &, … Jiménez, J. (2018). Toward reliable population estimates of wolves by combining spatial capture-recapture models and non-invasive DNA monitoring. *Scientific Reports*, *8*(1), 2177. https://doi.org/10.1038/s41598-018-20675-9

Lukacs, P. M., & Burnham, K. P. (2005). Review of capture-recapture methods applicable to noninvasive genetic sampling: REVIEW OF DNA-BASED CAPTURE-RECAPTURE. *Molecular Ecology*, *14*(13), 3909–3919. https://doi.org/10.1111/j.1365-294X.2005.02717.x

Marra, P. P., Cohen, E. B., Loss, S. R., Rutter, J. E., & Tonra, C. M. (2015). A call for full annual cycle research in animal ecology. *Biology Letters*, *11*(8), 20150552. https://doi.org/10.1098/rsbl.2015.0552

Muneza, A. B., Linden, D. W., Montgomery, R. A., Dickman, A. J., Roloff, G. J., Macdonald, D. W., & Fennessy, J. T. (2017). Examining disease prevalence for species of conservation concern using non-invasive spatial capture–recapture techniques. *Journal of Applied Ecology*, *54*(3), 709–717. https://doi.org/10.1111/1365-2664.12796

O'Brien, S., Robert, B., & Tiandry, H. (2005). Consequences of violating the recapture duration assumption of mark–recapture models: A test using simulated and empirical data from an endangered tortoise population. *Journal of Applied Ecology*, *42*(6), 1096–1104. https://doi.org/10.1111/j.1365-2664.2005.01084.x

O'Connell, A. F., Nichols, J. D., & Karanth, K. U. (2010). *Camera traps in animal ecology: Methods and analyses*. New York, NY: Springer Science & Business Media.

Otis, D. L., Burnham, K. P., White, G. C., & Anderson, D. R. (1978). Statistical inference from capture data on closed animal populations. *Wildlife Monographs*, *62*, 133.

Plummer, M. (2003). JAGS: A program for analysis of Bayesian graphical models using Gibbs sampling. In *Proceedings of the 3rd international workshop on distributed statistical computing* (Vol. 124, p. 125). Vienna. Retrieved from https://www.r-project.org/conferences/DSC-2003/Drafts/Plummer.pdf

Pollock, K. H., Nichols, J. D., Brownie, C., & Hines, J. E. (1990). Statistical inference for capture-recapture experiments. *Wildlife Monographs*, *107*, 3–97.

Promislow, D. E. L., & Harvey, P. H. (1990). Living fast and dying young: A comparative analysis of life-history variation among mammals. *Journal of Zoology*, *220*(3), 417–437. https://doi.org/10.1111/j.1469-7998.1990.tb04316.x

R Core Team (2017). R: A language and environment for statistical computing. R Foundation for Statistical Computing, Vienna, Austria. URL https://www.R-project.org/.

Roon, D. A., Waits, L. P., & Kendall, K. C. (2005). A simulation test of the effectiveness of several methods for error-checking non-invasive genetic data. *Animal Conservation*, *8*(2), 203–215. https://doi.org/10.1017/S1367943005001976

Rota, C. T., Fletcher, R. J. Jr, Dorazio, R. M., & Betts, M. G. (2009). Occupancy estimation and the closure assumption. *Journal of Applied Ecology*, *46*(6), 1173–1181. https://doi.org/10.1111/j.1365-2664.2009.01734.x

Rowan, W. (1938). Light and seasonal reproduction in animals. *Biological Reviews*, *13*(4), 374–401. https://doi.org/10.1111/j.1469-185X.1938.tb00523.x

Royle, J. A. (2011). Hierarchical spatial capture–recapture models for estimating density from trapping arrays. In A. F. O'Connell, J. D. Nichols, & K. U. Karanth (Eds.), *Camera traps in animal ecology* (pp. 163–190). Tokyo: Springer Japan. https://doi.org/10.1007/978-4-431-99495-4_10

Royle, J. A., Chandler, R. B., Sollmann, R., & Gardner, B. (2013). *Spatial capture-recapture*. Cambridge, UK: Academic Press.

Royle, J. A., & Dorazio, R. M. (2012). Parameter-expanded data augmentation for Bayesian analysis of capture–recapture models. *Journal of Ornithology*, *152*(2), 521–537. https://doi.org/10.1007/s10336-010-0619-4

Royle, J. A., Fuller, A. K., & Sutherland, C. (2017). Unifying population and landscape ecology with spatial capture-recapture. *Ecography*, *41*(3), 444–456. https://doi.org/10.1111/ecog.03170

Royle, J. A., & Young, K. V. (2008). A hierarchical model for spatial capture–recapture data. *Ecology*, *89*(8), 2281–2289. https://doi.org/10.1890/07-0601.1

Sollmann, R., Furtado, M. M., Gardner, B., Hofer, H., Jácomo, A. T. A., Tôrres, N. M., & Silveira, L. (2011). Improving density estimates for elusive carnivores: Accounting for sex-specific detection and movements using spatial capture–recapture models for jaguars in central Brazil. *Biological Conservation*, *144*(3), 1017–1024. https://doi.org/10.1016/j.biocon.2010.12.011

Stearns, S. C. (1992). *The evolution of life histories* (Vol. 249). Oxford, UK: Oxford University Press.

Stenglein, J. L., Waits, L. P., Ausband, D. E., Zager, P., & Mack, C. M. (2011). Estimating gray wolf pack size and family relationships using noninvasive genetic sampling at rendezvous sites. *Journal of Mammalogy*, *92*(4), 784–795. https://doi.org/10.1644/10-MAMM-A-200.1

Woodruff, S. P., Johnson, T. R., & Waits, L. P. (2016). Examining the use of fecal pellet morphometry to differentiate age classes in Sonoran pronghorn. *Wildlife Biology*, *22*(5), 217–227. https://doi.org/10.2981/wlb.00209

SUPPORTING INFORMATION

Additional supporting information may be found online in the Supporting Information section at the end of the article.

How to cite this article: Dupont P, Milleret C, Gimenez O, Bischof R. Population closure and the bias-precision trade-off in spatial capture–recapture. *Methods Ecol Evol*. 2019;10:661–672. https://doi.org/10.1111/2041-210X.13158